ENVIRONMENTAL BARRIER COATINGS FOR THE ENERGY EFFICIENT HEAT ENGINES PROGRAM

FINAL REPORT

For work performed from
June 1, 2001 to October 31, 2004

Work Performed Under
Cooperative Agreement No. DE-FC36-01CH11086

Prepared for
United States Department of Energy

by
Katherine T. Faber, Principal Investigator
Northwestern University

January 31, 2005

DISCLAIMER

ABSTRACT

This program aimed to develop a fundamental understanding of the microstructural, mechanical, and chemical properties of Ta_2O_5-based coatings for Si_3N_4 (AS800) substrates and optimize such coatings for environmental barriers. The program consisted of three tasks: processing of Ta_2O_5 coatings, phase and microstructural development, and life-limiting phenomena. Northwestern University formed a cross-functional team with Lehigh University, Honeywell Inc., and Oak Ridge National Laboratory.

The major accomplishments are:

- Conditions for the plasma spray of Ta_2O_5 and its alloys were optimized to provide maximum density and thickness.
- Adherent small particle plasma spray coatings of Ta_2O_5 can be routinely prepared.
- Ta_2O_5 can be stabilized against its disruptive phase transformation to1400°C by the addition of one or more oxides of Al, La, and/or Nb.
- Residual stresses in the Ta_2O_5 coatings were measured using X-rays and changed with thermal exposure.
- Properly doped coatings are more resistant against thermal cycling than undoped coatings, and can be cycled many thousand times without spallation.
- Water vapor testing in the ORNL Keiser Rig of adherent coatings showed that undoped Ta_2O_5 is not an effective barrier at preventing chemical changes to the AS800.
- Limited water vapor testing of doped and adherent coatings, which had successfully survived many thermal cycles, showed that in the water vapor environment, de-cohesion may occur.

PROJECT SUMMARY

Development of environmental barrier coatings (EBC) for the protection of silicon-based ceramics designed for use in gas turbine engines has been ongoing for over a decade. EBCs serve to shield the ceramic components from harmful gas turbine environment species, such as water vapor, which volatilize the protective silica layer that forms on silicon carbide and silicon nitride. Without protection, silicon-based ceramic components have exhibited severe surface recession which compromises their long-term use in gas turbines.

An effective EBC must prevent recession and degradation while not compromising the mechanical properties of the ceramic component over the desired lifetime. The coating material must be resistant to the gas turbine environment and must adhere well to the ceramic component. In addition, it should minimize harmful species from reaching the underlying ceramic, and/or prevent the volatilization product from leaving the surface of the substrate. Diffusion through the coating or exposure of the gas turbine environment to the ceramic through open porosity or cracking should be prevented. Macro-stresses, which could be a result of coefficient of thermal expansion mismatch with the substrate, and micro-stresses, which could result in materials with anisotropic coefficient of thermal expansions, should be minimized to prevent cracks in the coating.

The goal of this program was to develop a fundamental understanding of the microstructural, mechanical, and chemical properties of Ta_2O_5-based coatings for Si_3N_4 substrates and optimize such coatings for environmental barriers. The program consisted of three tasks

Task 1: Processing of Ta_2O_5 coatings
Task 2: Phase and microstructural development
Task 3: Life limiting phenomena

Northwestern University formed a cross-functional team for this environmental barrier coating research. Team members consisted of Lehigh University, a leader in research on microstructure and mass transport in ceramics, and Honeywell Inc., an industrial leader in ceramic and coating research and development and a supplier of silicon nitride ceramic engine components. Related studies at high temperatures and water vapor pressures were conducted at Oak Ridge National Laboratory, but are reported in an independent document. Northwestern University, Honeywell, Inc. and Lehigh University participants are listed in Appendix A.

The efforts undertaken and results obtained in each of the above tasks will be discussed in the following sections. Publications and presentations of this work are listed in Appendix B.

Task 1: Processing of Ta_2O_5 coatings

Honeywell supplied Northwestern with process information, AS800 specimens, and pre-reacted Ta_2O_5 alloy powders. Process information relating to Honeywell's experience with applying plasma sprayed Ta_2O_5 to AS800 was transferred to Northwestern, including information regarding preferred substrate temperature conditions and their experience with particle sizes and the pre-reaction of powder.

Approximately 150 coupons with one surface as-processed were cut from AS800 billets. Several sample geometries were prepared to accommodate both Tasks 1 and 3. In the latter, substrates were prepared for (a) thermal cycling at Honeywell, (b) Keiser rig testing at ORNL, and (c) burner rig testing at IKTS (Fraunhofer Institute for Keramic Technology and Sintering, Dresden , Germany). However, burner rig coupons were prepared, but not tested. Most specimens were heat treated at 1250°C for 0.5 h in air to stabilize the grain boundary oxynitride phase against the possibility of a disruptive volume expansion during exposure to the intermediate temperatures which the samples were subjected to during plasma spraying[1]. However early samples were not given this treatment and the low strengths noted for those samples as part of the Keiser Rig tests at ORNL may have been as a result of damage to changes in the un-stabilized AS800 grain boundary phases during SPPS.

Using a D-optimal design of experiments, small particle plasma-sprayed (SPPS) processing variables were optimized to maximize coating density. It was anticipated that the maximum density would minimize permeability of water vapor in use. The effect of processing variable on coating thickness was also determined as an indication of spray efficiency. For pure Ta_2O_5 powders, a multiple regression model for coating porosity (P) was found to be:

$$\frac{1}{P} = -0.340 + 1.49 \times 10^{-3} R - 2.40 \times 10^{-6} R^2 + 0.0217 A + 0.0950 O - 4.33 \times 10^{-3} (A * O)$$

where R is robot scan rate, A is injector angle and O is injector offset. Note the interaction effects between angle and offset (A*O). Plasma-spray conditions for coatings optimized for thickness are shown in Table 1. The predicted means for thickness and porosity computed from these models are 100 microns and 2.70%, and the 95% confidence intervals for the means are 90 to 113 μm for thickness and 2.24% and 3.41% for porosity.

Table 1. Spraying conditions for Ta_2O_5 coatings optimized for minimal porosity.

Robot scan rate (R)	315 mm/min
Injector angle (A)	0°
Injector offset (O)	5 mm
Carrier gas flow (CF)	3 slm
Power feeder disc speed (DS)	0.4 rpm
Plasma gun power (P)	40 kW
Total gas flow (TF)	44 slm
% Hydrogen in plasma gas (%H)	25 %

[1] In the intermediate temperature range (~700-1000C), the microstructure is too rigid to allow the stress induced by the oxidation of oxinitride grain boundary phases to be relieved through viscous/plastic flow. This can result in cracking of the material under certain circumstances. For further discussion of this mechanism see, e.g., Patel, J.K., et al., "The low temperature oxidation problem in yttria-densified silicon nitride ceramics", Br. Ceram Trans. J. 87, 70-73, 1988.

Several confirmation runs were completed at the settings shown in Table 1, with results that closely match the values of porosity predicted by the above equation. The average porosity for seven specimens was 2.76%, with a 95% confidence interval for the mean of 1.7% to 3.8%. The one-sided t-test shows that one cannot reject the null hypothesis (mean = 2.70%, P = 0.90). Figure 1 shows an optimized coating that has an average thickness of 85 μm and approximate porosity of 1.5% (the smallest value found), as measured by stereological methods.

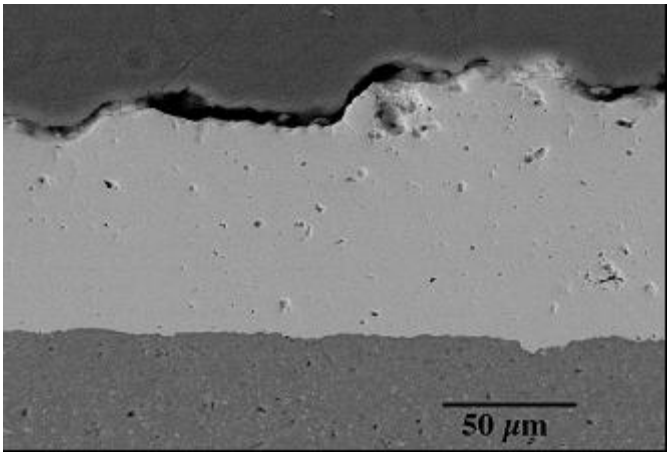

Figure 1. Scanning electron micrograph of optimized Ta_2O_5 of appropriate thickness.

1.1 Preparation of Ta_2O_5 alloyed coatings

Because of the important role of Al_2O_3 and $AlTaO_4$ in grain boundary pinning of Ta_2O_5 described under Task 2, Honeywell investigated routes to prepare the following compositions:

- Pure $AlTaO_4$ phase (1Al:1Ta) that could be used for mixing with pure Ta_2O_5 and with Ta_2O_5 + 1 wt% Al_2O_3 for plasma spray trials.
- Ta_2O_5 + 3 wt% Al_2O_3 (above expected solubility limit of Al in Ta_2O_5) ($AlTaO_4$ formed during heat treatment) that could be used directly for plasma spray trials.
- Ta_2O_5 + 2 wt% Al_2O_3 (just above expected solubility limit of Al in Ta_2O_5) (trace $AlTaO_4$ formed during heat treatment) that could be used directly for plasma spray trials.
- Ta_2O_5 + 1 wt% Al_2O_3 (just below expected solubility limit of Al in Ta_2O_5 that could be used directly for plasma spray trials or for mixing with pure $AlTaO_4$ for plasma spray trials.

Mixtures of Ta_2O_5 (First Reaction, Inc) with appropriate amounts of either aluminum nitrate or gamma (γ) alumina as the aluminum source, and heat-treated the mixtures in air at various temperatures (5 hrs at temp, 10°C/min heating/cooling rates).

X-ray diffraction analysis shows varying degrees of reaction depending on the temperature and source of alumina. The degree of reaction was assessed by evaluating the areas beneath the strongest peaks for β-Ta_2O_5 (JCPDS# 25-0922) and $AlTaO_4$ (JCPDS# 25-1490).

Equal weight was given to both phases in this evaluation. The percentage $AlTaO_4$ was evaluated as follows:

$$\% AlTaO_4 = \text{Area } AlTaO_4 / (\text{Area } AlTaO_4 + \text{Area } \beta\text{-}Ta_2O_5) * 100.$$

Tables 2 and 3 summarize the % $AlTaO_4$ seen in the mixtures that were heat-treated at varying temperatures. Table 2 shows a summary for heat treatments made using aluminum from aluminum nitrate. Table 3 shows a summary for heat treatments made using aluminum from γ alumina.

Table 2: Summary of the % $AlTaO_4$ content (as determined by ratios of the areas beneath the strongest $AlTaO_4$ and β-Ta_2O_5 XRD peaks) in Ta_2O_5-aluminum nitrate mixtures which were heat-treated at varying temperatures.

Temp (°C)	1Al:1Ta	3 wt% Al	2 wt% Al	1 wt% Al
1200	44	6	2	0
1300	76	8	6	6
1350	91	17	4	0
1400	95	12	4	2
1500	81	10	8	0

Table 3: Summary of the % $AlTaO_4$ content (as determined by ratios of the areas beneath the strongest $AlTaO_4$ and β-Ta_2O_5 XRD peaks) in Ta_2O_5-γ-Al_2O_3 mixtures which were heat-treated at varying temperatures.

Temp (°C)	1Al:1Ta	3 wt% Al	2 wt% Al	1 wt% Al
1200	24	2	1	0
1300	32	5	1	0
1350	45	7	3	0
1400	60	7	3	0

Initial examination of the results indicate that nearly-pure $AlTaO_4$ can be formed by the proper heat treatment of Ta_2O_5 and aluminum nitrate mixtures (1Al: 1Ta) (for example at 1400°C). A lesser degree of conversion at a given temperature was seen in the γ-Al_2O_3 mixtures. The reason for the decrease in the $AlTaO_4$:β-Ta_2O_5 ratio at 1500°C in the nitrate mixtures is uncertain.

For the 1, 2, and 3 wt% mixtures, suitable heat treatment conditions were determined for preparing "pre-reacted" powders for plasma spraying, in which the β-Ta_2O_5 phase was saturated with aluminum. The results generally confirm the results reported earlier by Lehigh (Quarterly Report 4) that aluminum additions up to 1 wt% are held in Ta_2O_5-Al solid solution and that by 3 wt% $AlTaO_4$ significant precipitation can be seen. In addition, these results indicate that the

$AlTaO_4$ formation occurs to a limited extent for 2 wt% Al additions. The results for the 1wt% nitrate additions also suggest that under certain conditions $AlTaO_4$ may be seen in the 1% mixtures, although due to difficulties encountered with nitrate processing, that observation should be further examined.

In addition to the powders described above, Honeywell also supplied Northwestern with the following pre-reacted powders for plasma spraying:

- Ta_2O_5 with 5 wt% Al_2O_3 (1400°C/5 hour in air) (prepared by Honeywell under earlier internal efforts)
- Ta_2O_5 with 3 wt% Al_2O_3 + 3wt % La_2O_3 (1400°C/5 hour in air) (prepared by Honeywell under internal efforts)
- Ta_2O_5 + 1.5 wt%Al_2O_3
- Ta_2O_5 + 1.5 wt%Al_2O_3 + 1.5 wt% La_2O_3

The latter two powders were made by milling high purity oxides (First Reaction, Baikowski-Gamma type, and American Elements, respectively) in alcohol, evaporating the alcohol, and calcining the mixture at 1350°C for 5hrs (5°C/minute heating rate).

Plasma spray parameters for alloyed powders were identical to those used on pure Ta_2O_5 and were previously optimized. The substrates (5 cm x 2.5 cm x 0.3 cm) were ultrasonically cleaned in propanol for 5 minutes prior to spraying. The substrate was held against a ceramic plate containing heating elements which preheated the AS800 prior to plasma spraying. Samples prepared under this effort were used for static heat treatments, thermal cycling, Keiser Rig experiments and residual stress measurements.

Task 2: Phase and Microstructural Development

This task was to identify appropriate dopants and/or second phases which would enhance the effectiveness of Ta_2O_5 as an environmental barrier coating, in terms of microstructural stability, inhibition of grain boundary transport kinetics, stabilization of the β-Ta_2O_5 phase to higher temperatures and improved thermal expansion match with the Si_3N_4 substrate. A large portion of the effort focused on the influence of dopants of Al_2O_3, La_2O_3, and Nb_2O_5. This work was largely conducted by investigators at Lehigh University identified in Appendix A.

Samples for these studies were prepared as pellets using conventional ceramic powder mixing, pressing and sintering techniques. Results from these studies were often incorporated into powder processing strategies at Honeywell and were plasma-sprayed at Northwesten University for further testing.

2.1 Phase transformation from orthorhombic (β) to tetragonal (α) Ta_2O_5

It was observed that for undoped Ta_2O_5, extensive cracking of the pellets occurred during sintering due to the volume expansion associated with the transformation from the orthorhombic (β) to tetragonal (α) phase. We have estimated the magnitude of the volume expansion to be of the order of 6.2 to 8.6%. High temperature in-situ X-ray diffraction studies were carried out at Alfred University to further study the transformation. Diffraction patterns of undoped Ta_2O_5

during heating and cooling are given in Figure 2. The number by each individual pattern represents the temperature at which the X-ray scan was carried out; the letter "d" indicates cooling down. It can be seen that from room temperature (50°C) up to 1100°C, the patterns correspond to the orthorhombic (β) phase. At 1300°C, however, a new peak emerged at two-theta ~ 36.57° (indicated by an arrow), which is the strongest distinguishable peak for the tetragonal (α) phase. This indicates the occurrence of the phase transformation from β-to-α.

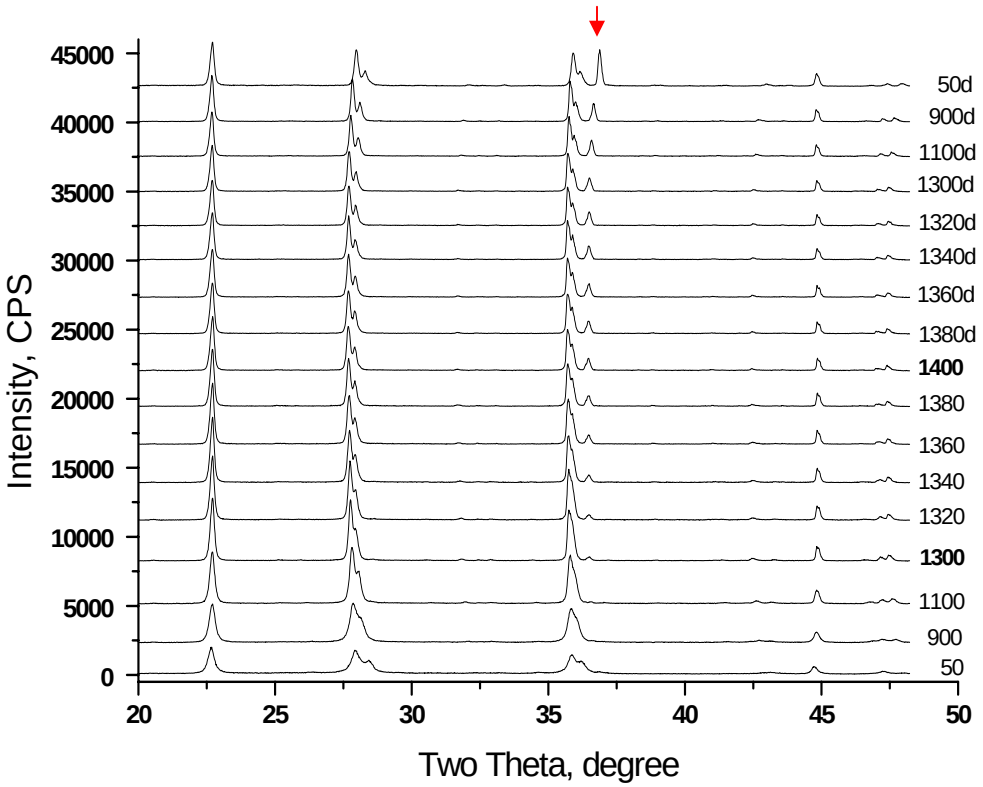

Figure 2. X-ray diffraction patterns of an undoped Ta_2O_5 powder, as milled. The arrow indicates the position of a peak associated with the formation of the tetragonal phase.

The magnitude of the α-peak grew as the temperature increased, showing an increase in the degree of phase transformation. During cooling from 1400°C, the α-peak remained and the peak intensity continued to increase down to room temperature. This observation conflicts with previous reports in the literature stating that the β-to-α phase transformation occurs at ~1360°C and is reversible. The shift of the α-peak to the right was due to thermal expansion and fast cooling (20 and 60°C/min above and 700°C).

2.2 Effect of Al_2O_3 additions

The influence of Al_2O_3 additions on the phase transformation is illustrated in Figure 3, which compares the microstructures of Ta_2O_5 samples sintered at 1300°C for 99 hours. It is seen that whereas microcracking occurred in the undoped Ta_2O_5 (Fig. 3(A)), samples doped with 3 wt% Al_2O_3 were crack-free. At this dopant level, the solubility limit is exceeded, hence the presence of fine second phase particles ($AlTaO_4$) located at the grain boundaries (Fig. 3(B)).

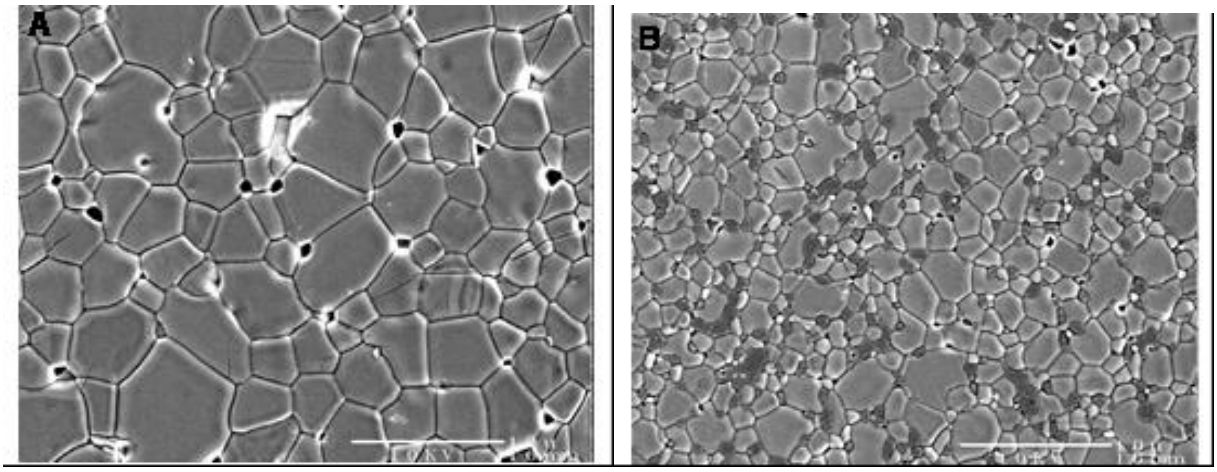

Figure 3. Microstructures of (A) undoped and (B) 3 wt% Al_2O_3-doped Ta_2O_5 sintered at 1300°C for 99 hours.

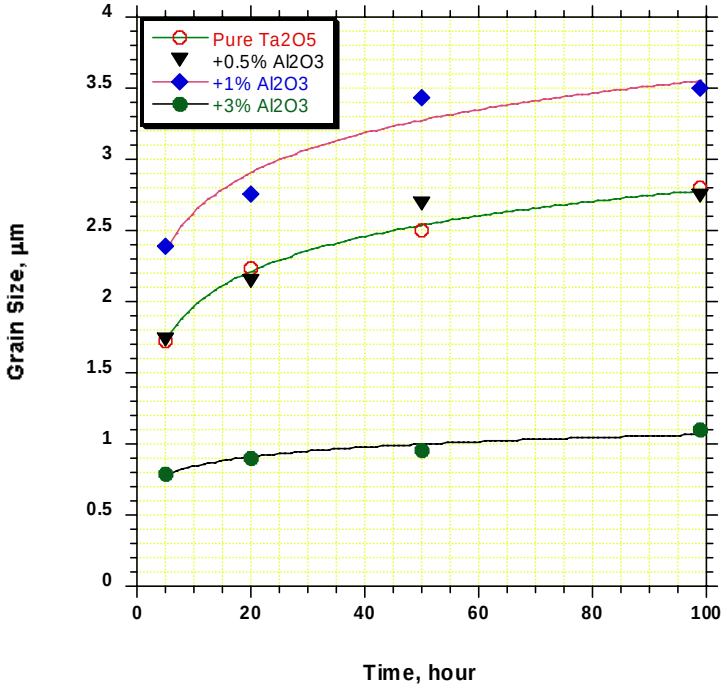

Figure 4. Grain size data of Ta_2O_5 doped with various amounts of Al_2O_3, sintered at 1300°C.

The average grain size of Ta_2O_5 samples doped with 0 – 3 wt% Al_2O_3, and fired at 1300°C for different periods of time, are represented in Figure 4. At the 0.5% dopant level, the grain size (and microstructure) were very similar to that of the undoped Ta_2O_5. However, the sample doped with 1% Al_2O_3 exhibited the largest grain size of the four samples. Figure 4 clearly shows that the highest dopant level studied (≥3%) resulted in the finest grain size, due to pinning by the $AlTaO_4$ second phase particles.

2.3 Effect of La_2O_3 additions

The addition of La_2O_3 was also found to suppress the β-to-α phase transformation. The microstructure of a Ta_2O_5 sample doped with 1.5% La_2O_3 (fired at 1340 °C for 10 hours) is shown in Figure 5. It was observed that as the La_2O_3 content increased, the density of the sintered samples decreased. Note that for an undoped Ta_2O_5 sample, the same heat-treatment resulted in the sample being broken into small fragments. A distinguishing feature of the microstructures of the La_2O_3-doped samples is the presence of elongated grains of the second phase $LaTa_7O_{19}$.

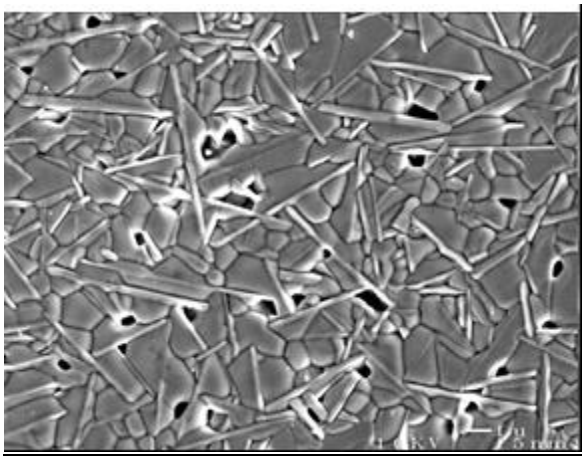

Figure 5. Microstructure of 1.5 wt% La_2O_3-doped Ta_2O_5 sintered at 1340°C for 10 hours.

2.4 Effect of Nb_2O_5 additions

The microstructures of the fired samples containing varying amounts (1 – 5 wt%) of Nb_2O_5 are given in Figure 6. Microcracking occurred in all samples, indicating that the β-to-α phase transformation had taken place during firing. Furthermore, in contrast to the results for Al_2O_3 and La_2O_3 containing compositions, Nb_2O_5 additions (for corresponding dopant levels), did not result in the formation of second phase particles.

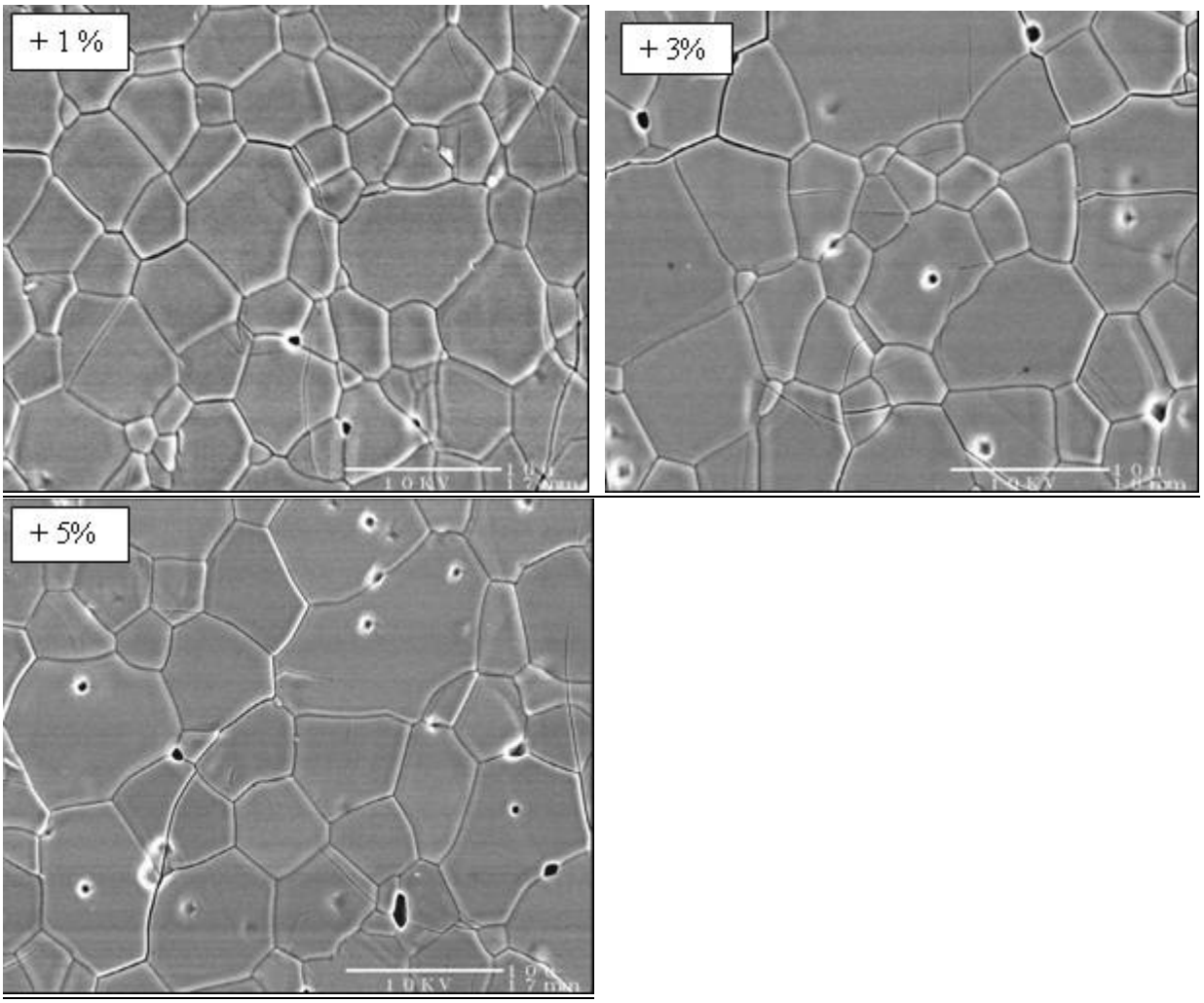

Figure 6. Microstructures of 1, 3 and 5 wt% Nb_2O_5 doped Ta_2O_5 fired at 1380°C for 5 hrs. Note that microcracking is common in all samples indicating that the β-to-α phase has occurred to some extent during firing.

2.5 Co-doping of Ta_2O_5 with Al_2O_3/La_2O_3

Representative microstructures of samples of Ta_2O_5 co-doped with 2 wt% γ-Al_2O_3 and 1 wt% La_2O_3, are depicted in Figure 7. The elongated grains are a La_2O_3-rich phase ($LaTa_7O_{19}$) and the small dark particles are an Al_2O_3-rich phase ($AlTaO_4$). The second phase particles are uniformly distributed in the Ta_2O_5 matrix. The combined addition of Al_2O_3 and La_2O_3 worked together to effectively stabilize the low-temperature crystal structure (β) and refine the Ta_2O_5 microstructure. Only limited microcracking was observed in the sample fired at 1450°C for 5 hours (Figure 7(C)).

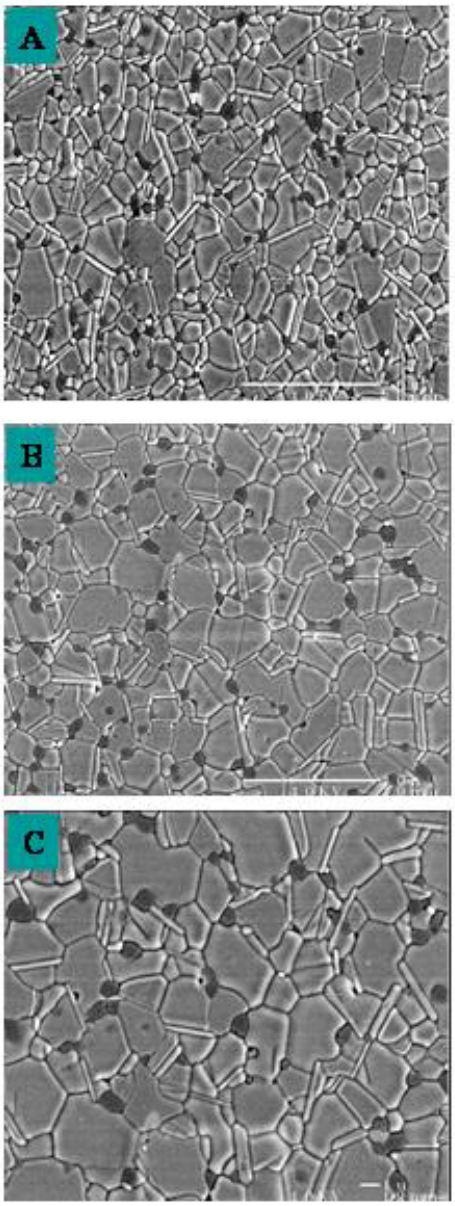

Figure 7. Microstructures of Ta_2O_5 doped with 2 wt% γ-Al_2O_3 and 1 wt% La_2O_3, fired at (A) 1350°C, (B) 1400°C and (C) 1450°C for 5 hours.

2.6 Thermal Expansion of Ta_2O_5 co-doped with Al_2O_3 and Nb_2O_5

The thermal expansion behavior of Ta_2O_5 co-doped with Al_2O_3 and Nb_2O_5 was measured and the data are presented in Figure 8. As expected, the co-doping of Nb_2O_5 and Al_2O_3 was beneficial with regard to matching the thermal expansion coefficients of AS800 Si_3N_4 and the coating material. It can be seen that the expansion curves of the samples doped with 5 and 7 wt% Nb_2O_5 are almost identical, and closely match that of the AS800. The measured thermal expansion coefficients for the Ta_2O_5 co-doped with Al_2O_3 and Nb_2O_5, and some related materials are listed in Table 4.

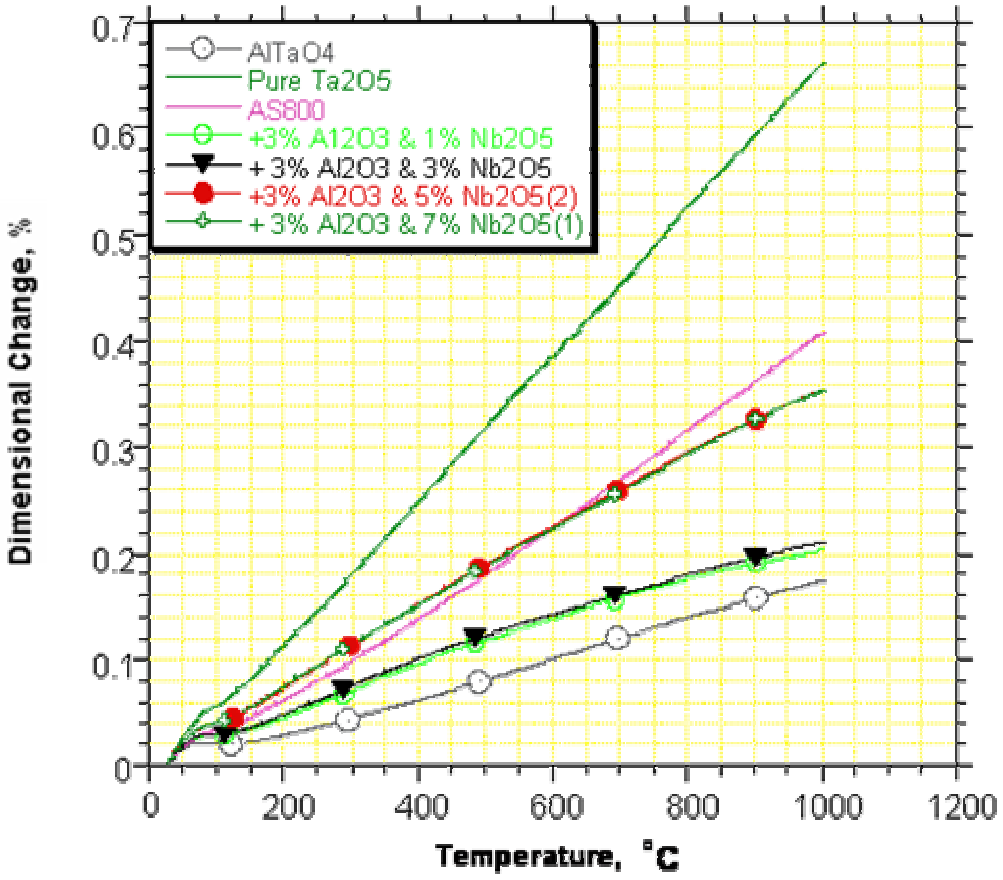

Figure 8. Thermal expansion behavior of Ta_2O_5 co-doped with 3 wt% Al_2O_3 and various amounts of Nb_2O_5. Data for $AlTaO_4$ and AS800 Si_3N_4 are also plotted for comparison.

Table 4. Thermal expansion coefficients of Ta_2O_5, $AlTaO_4$ and AS800 Si_3N_4 ceramics in a temperature range up to 1000°C.

Material	Thermal Expansion Coefficient
$AlTaO_4$	1.84×10^{-6}
Ta_2O_5 doped with 3% Al_2O_3	2.42×10^{-6}
Ta_2O_5 doped with 3% Al_2O_3 and 5% or 7% Nb_2O_5	3.54×10^{-6}
AS800 Si_3N_4	4.33×10^{-6}
Pure Ta_2O_5	6.72×10^{-6}
Ta_2O_5 doped with 3% Al_2O_3 and 1% or 3% Nb_2O_5	2.14×10^{-6}

Task 3: Life Limiting Phenomena

To characterize the suitability of SPPS coatings for engine applications which contain water vapor in the combustion atmosphere, Ta_2O_5-coated AS800 was exposed to a series of static and cyclic heat treatments, cyclic steam exposures at Honeywell, and Keiser Rig exposures (reported on by Oak Ridge National Laboratory). Materials which underwent these exposures were evaluated for microstructural changes and for residual stress changes. In the case of cyclic steam exposures, changes in mass were also evaluated. The results of those tests are presented here.

3. 1 Thermal cycling tests

Using a high temperature cyclic oxidation furnace (procured outside the scope of this program using Honeywell capital resources), Honeywell completed cyclical heat-treatment tests on a number of Northwestern-sprayed samples of uncoated AS800 and coatings of pure Ta_2O_5, Ta_2O_5 + 2 wt% Al_2O_3, Ta_2O_5 + 3 wt% Al_2O_3, Ta_2O_5 + 5 wt% Al_2O_3, and Ta_2O_5 + 3 wt% Al_2O_3 + 3 wt% La_2O_3. Three separate rounds of tests were conducted as described below. In all cases the thermal cycle was as follows: 25 minutes in the furnace, 5 minutes out of the furnace in forced room temperature air stream. A picture of the furnace used to conduct the thermal cycling is shown in Appendix C.

Round 1

The first set of twenty-five samples was thermal cycled for up to 3358 cycles at either 1200 °C and/or 1315 °C. A summary of the samples and conditions is shown in Appendix D. In general, all coatings performed well under thermal cycling conditions, with the exception of some undoped Ta_2O_5 coatings, and all of the Ta_2O_5 + 5 wt% Al_2O_3 coatings. Only the Ta_2O_5 + 3 wt% Al_2O_3 + 3 wt% La_2O_3 was seen to survive more than 3000 cycles to 1315°C. Following testing all samples were sent to Northwestern for further examination.

Photographs showing samples upon removal from the hot furnace are attached. Figure 9 shows a large group of samples after 2 thermal cycles to 1200°C. In this photograph, subsurface defects can be seen. It is uncertain as to the cause of these defects, but during continued cycling the coating at that region was seen to crack and spalled from the substrate. Figure 10 and Figure 11 show a small group of samples after more than 650 and 1315 cycles at 1315°C. In these photos, damage can be seen to progress on the edge of the Pure Ta_2O_5 coated-sample. No subsurface damage can be seen.

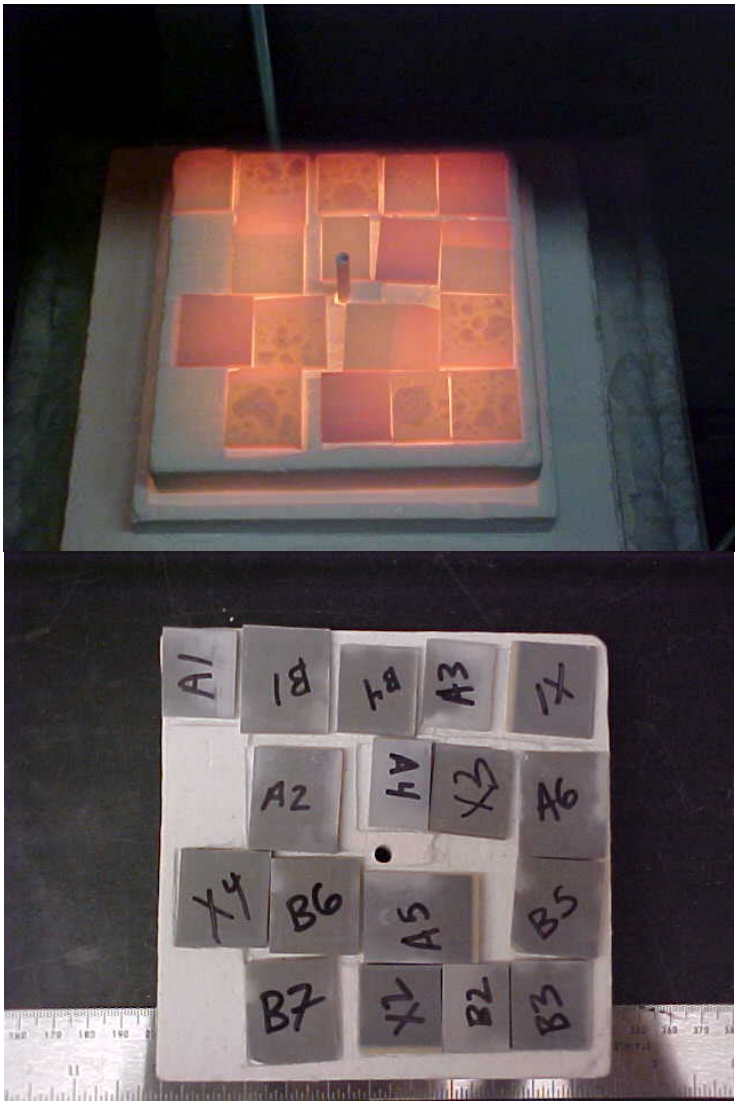

Figure 9. Upper photograph showing thermal cycling samples after 2 cycles at 1200°C, upon removal from furnace (samples hot). The non-uniform, mottled appearance indicates sub-surface delamination. Lower photograph gives sample number (see Appendix D) and scale.

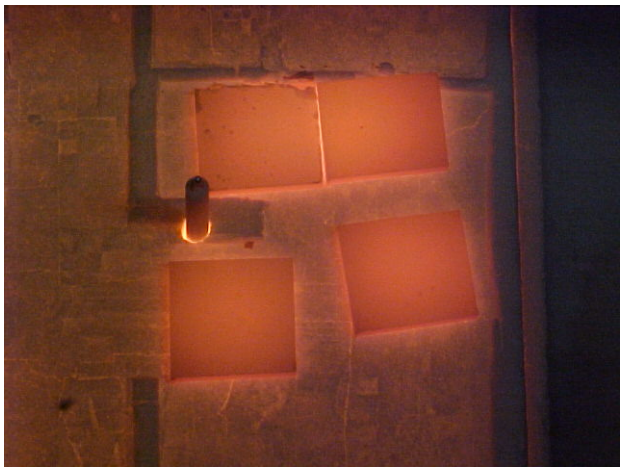

Figure 10. Thermal cycling samples after 770 cycles. Samples are approximately 25 x 25 mm. Samples shown are (clockwise from upper left): A7, C3, E1, D3 (see Appendix D). Sample A7 (pure Ta_2O_5) shows signs of delamination at the edges.

Figure 11. Thermal cycling samples after 1416 cycles. Samples are approximately 25 x 25 mm. Samples shown are (clockwise from upper left): A7, C3, E1, D3 (see Appendix D). Sample A7 (pure Ta_2O_5) shows signs of progressive delamination at the edges.

Round 2:

The second set of sixteen samples was thermal cycled for either 140, 490, or 1080 cycles between room temperature and 1200°C. All samples were plasma sprayed with either Ta_2O_5 + 1.5 wt% Al_2O_3 or Ta_2O_5 + 1.5 wt% Al_2O_3 + 1.5 wt% La_2O_3. A summary of the samples and conditions is shown in Appendix E. All samples survived testing without any noted delamination, and were sent to Northwestern so that they could be studied using the Argonne National Lab (ANL) Advanced Photon Source (APS) to determine the effect of thermal cycles on the residual stress state in the samples.

Round 3:

The third set of six samples was thermal cycled for 1000 cycles between room temperature and 1200 °C, followed by 1000 cycles between room temperature and 1315 °C. All samples were plasma sprayed with either Ta_2O_5 + 1.5 wt% Al_2O_3 or Ta_2O_5 + 1.5 wt% Al_2O_3 + 1.5 wt% La_2O_3. A summary of the samples and conditions is shown in Table 5 below. All samples survived testing without any noted delamination. Following thermal cycling, samples AL1 and ALLA1 were subjected to steam furnace testing as will be described in a later section. All other AL and ALLA samples were sent to Northwestern for further study and archiving.

Table 5: Summary log of thermal cycling samples from Round 3

Coating composition	**#cycles @ 1200°C**	**#cycles @ 1315°C**	**Results, observations**
Group AL: Ta_2O_5 + 1.5wt% Al_2O_3			
sample AL1	1000	1000	No delamination seen
sample AL2	1000	1000	No delamination seen
sample AL3	1000	1000	No delamination seen
sample AL4	1000	1000	No delamination seen
Group ALLA: Ta_2O_5+1.5wt% Al_2O_3+1.5wt% La_2O_3			
sample ALLA1	1000	1000	No delamination seen
sample ALLA2	1000	1000	No delamination seen

3.2 Residual stress measurements

X-ray diffraction measurements were conducted on both the statically heat-treated and thermally cycled samples using high-energy synchrotron radiation at the 1-ID (XOR-CAT) beam line of the Advanced Photon Source at Argonne National Laboratory. Diffraction data were used to determine residual stresses in the AS800 substrates and both phase evolution and residual stresses in the tantalum oxide coatings as a function of heat treatment. Residual stresses were also determined in as-received and thermally-cycled uncoated AS800 substrates. As-sprayed and heat-treated specimens were cross-sectioned to create 0.5-1 mm thick slices. The experiments

were conducted in transmission as illustrated in Figure 12, which afforded a through-the-thickness residual stress profile in 20 μm increments, in contrast to the reflection geometry which only provides residual stress assessment in the exterior tens of microns.

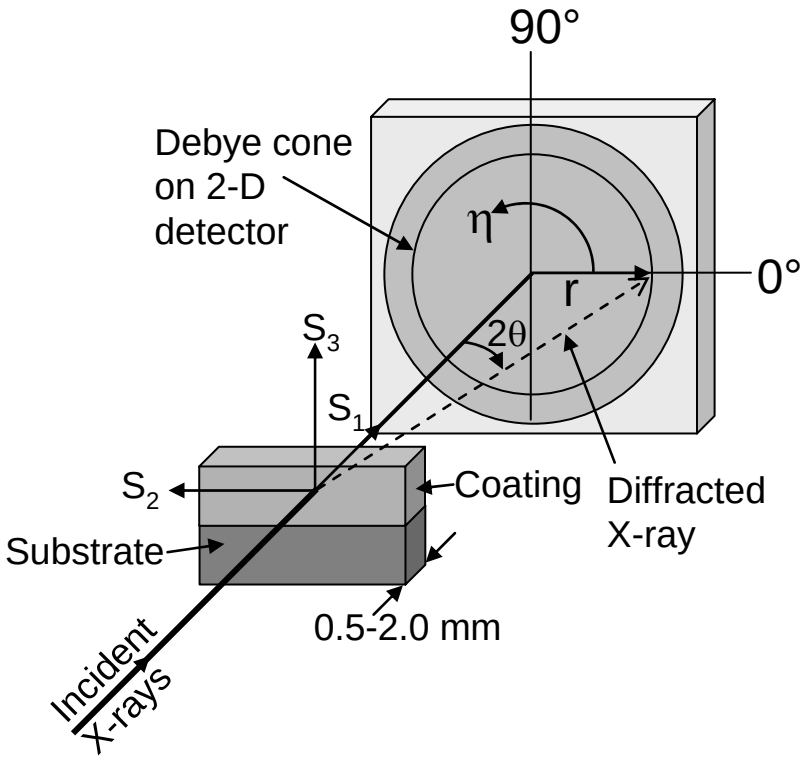

Figure 12. Schematic of the X-ray diffraction set up at the Advanced Photon source of Argonne National Laboratory for residual stress measurement.

AS800 was found to have compressive residual stresses near the surface due to a post-processing heat treatment. These stresses remained compressive regardless of the stress state of the coating although the stress profile with depth was found to change with additional heat treatment.

Though numerical analysis of the bulk properties of Ta_2O_5 and AS800 indicated that the coating should be in compression, as-sprayed coatings were measured to be in tension (Figure 13), most likely due to the non-equilibrium nature of the plasma-spray process. Tensile quenching stresses that developed due to shrinkage of individual splats during solidification had a significant effect on the residual stress state of the coating. In addition, as-sprayed coatings contained the high-temperature α-Ta_2O_5 phase which could also affect coating stresses. Heat treatments (static or cyclic) produced an equilibrium β-Ta_2O_5 coating with compressive stresses more consistent with numerically-predicted equilibrium thermal mismatch stresses, also shown in Figure 13. Vertical macro-cracking in as-sprayed coatings as well as buckling and microcracking in heat-treated coatings both led to a stress relaxation of residual stresses. Macro-cracks formed due to high tensile stresses after plasma spraying, but healed during initial heat

treatments. Buckling occurred in heat-treated coatings due to high compressive stresses, and was evident in cross-sections examined by scanning electron microscopy (Figure 14).

Microcracks resulted from grain growth in the Ta_2O_5 due to its anisotropic coefficient of thermal expansion. Though the cracks in the coating relieved stresses, they would be detrimental for an environmental barrier since they would provide a pathway for the gas turbine environment to reach the silicon nitride ceramic. Buckling can also lead to large scale spallation of the coating, also exposing the ceramic underneath. Hence, it was determined that pure Ta_2O_5 is not a viable coating in an EBC system for use with silicon nitride.

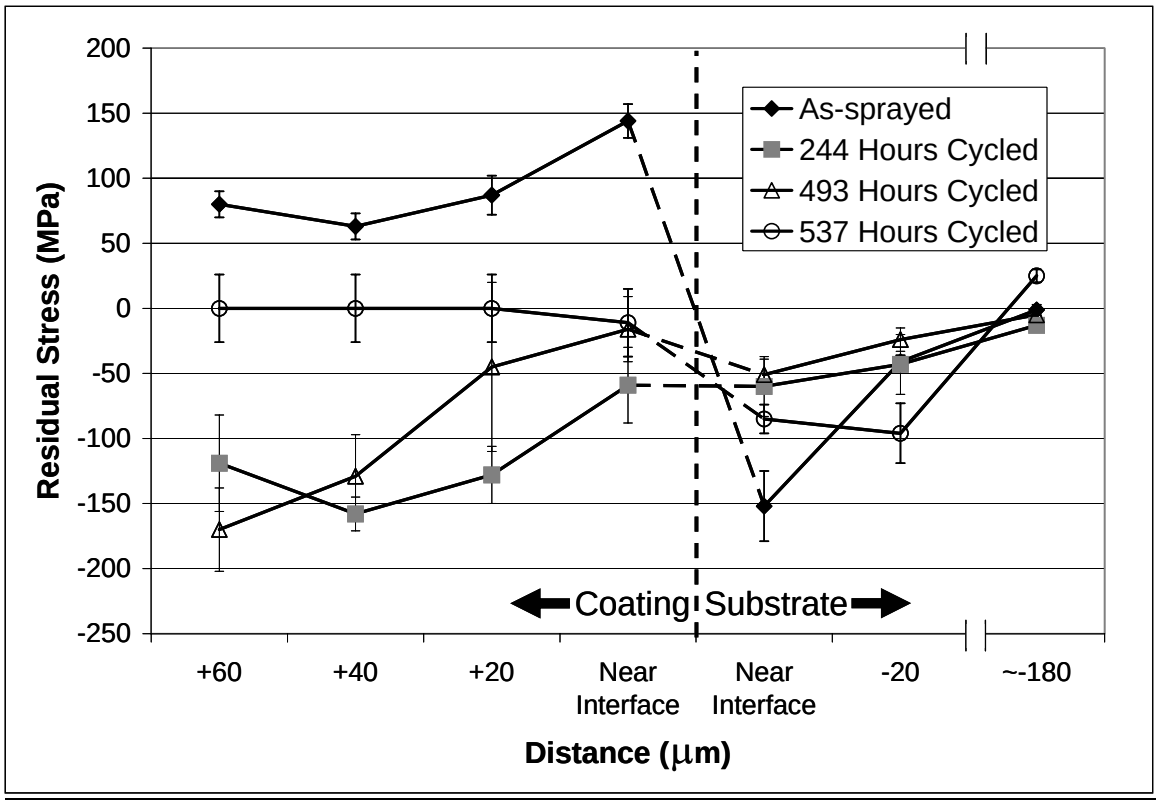

Figure 13. Residual stress results for as-sprayed and cyclically heat-treated (30 min. cycles to 1200°C in air) coatings on AS800.

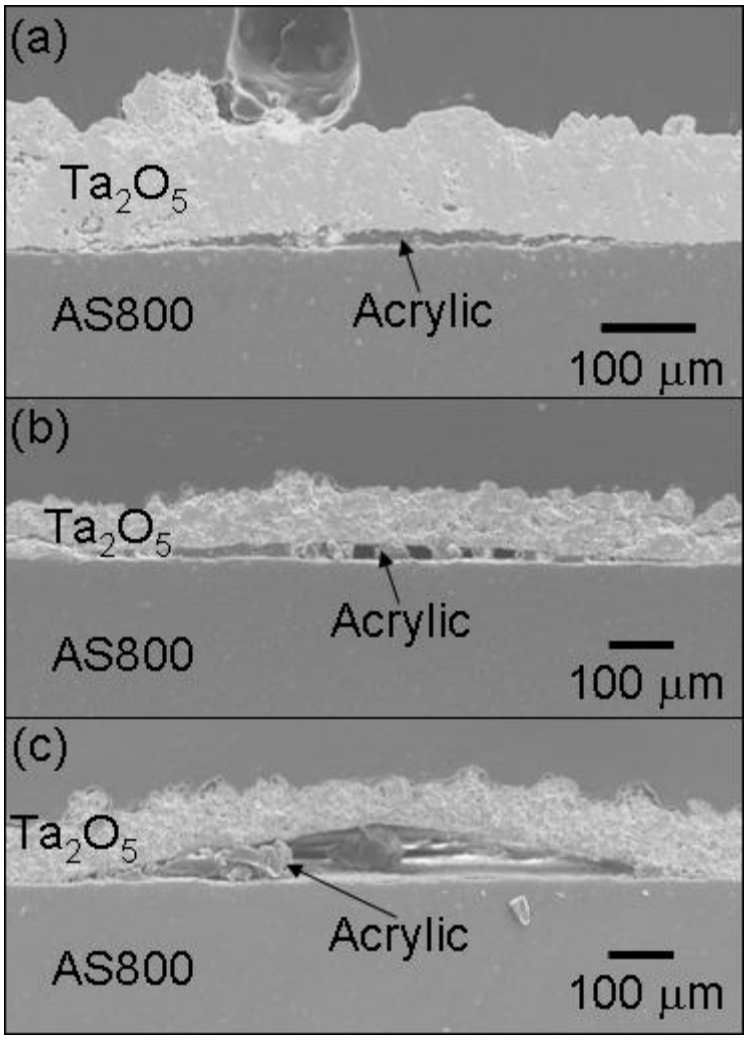

Figure 14. Micrographs showing buckling in coatings cyclically heat treated for (a) 72 hours, (b) 493 hours and (c) 537 hours. Some of the mounting acrylic, found between the coating and substrate, pulled out during polishing in (b) and (c).

Four compositions of alloyed powders of Ta_2O_5 containing Al_2O_3 or Al_2O_3/La_2O_3 were small particle plasma sprayed on AS800 and heat treated to 1200°C in air. Residual stresses in all these coatings were determined to be tensile indicating that the alloyed coatings had coefficients of thermal expansion that are higher than AS800. The alloying additions successfully reduced grain growth in the coatings, as displayed in Figure 15, and microcrack formation was eliminated in coatings containing La_2O_3. The Ta_2O_5 + 1.5 wt.% Al_2O_3 + 1.5 wt.% La_2O_3 alloy showed the most promise for use as an environmental barrier coating due to the microstructural stability, as evidenced by nearly invariant residual stress with heat treatment and lack of microcracking, shown in Figure 16. Exposure of Ta_2O_5 + 1.5 wt.% Al_2O_3 and Ta_2O_5 + 1.5 wt.% Al_2O_3 + 1.5 wt.% La_2O_3 coated AS800 samples to thermal cycling in air for 500 hours at 1200°C and 500 hours at 1315°C did not lead to spallation of the coatings.

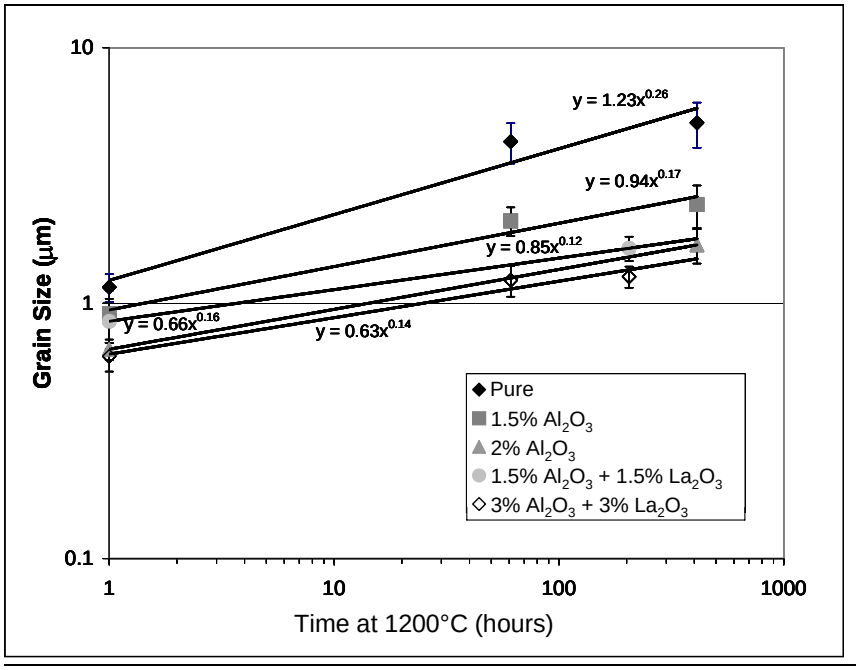

Figure 15. Grain size as a function of time at temperature for cyclically heat-treated pure and alloyed Ta_2O_5 coatings determined from stereology measurements. Error bars represent one standard deviation.

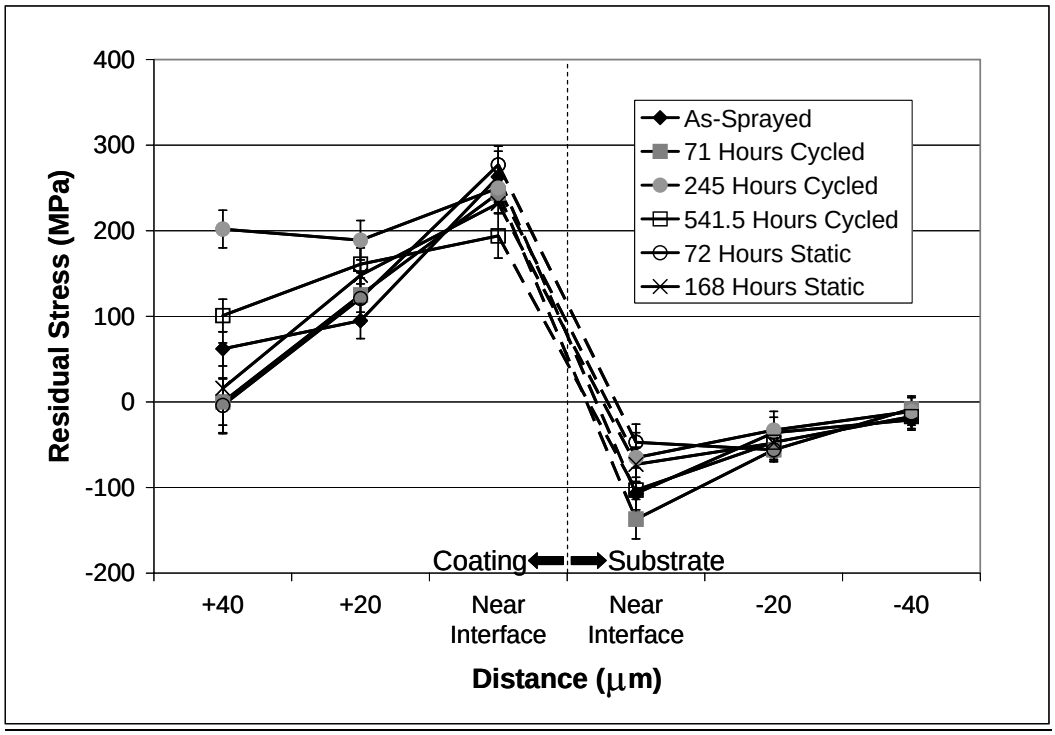

Figure 16. Residual stresses determined for as-sprayed and heat-treated coatings of Ta_2O_5 with 1.5 wt% Al_2O_3 + 1.5 wt% La_2O_3 on AS800 substrates.

3.3 Steam Furnace Testing

After samples (identified in Appendix D) had each been previously thermal cycled for 1000 cycles to 1200 °C then 1000 cycles to 1315°C without failure, samples AL1 and ALLA1 were supported on silicon nitride bars and put into a 76 mm diameter SiC tube furnace heated to 1315°C. Water was peristaltically pumped into one end at a flowrate of approximately 2.9 ml/min. Steam exited the furnace at either end. The estimated steam velocity was estimated to be approximately 2 meters per minute. Each end of the tube had a 6 mm diameter hole open to the laboratory atmosphere. Therefore the water vapor pressure was assumed to be approximately 1 atmosphere.

The specimens were removed periodically to assess mass change. The mass change results are shown in Figure 17. The coated samples were removed at 209 hours at which time complete delamination of the coating from the substrate was noted.

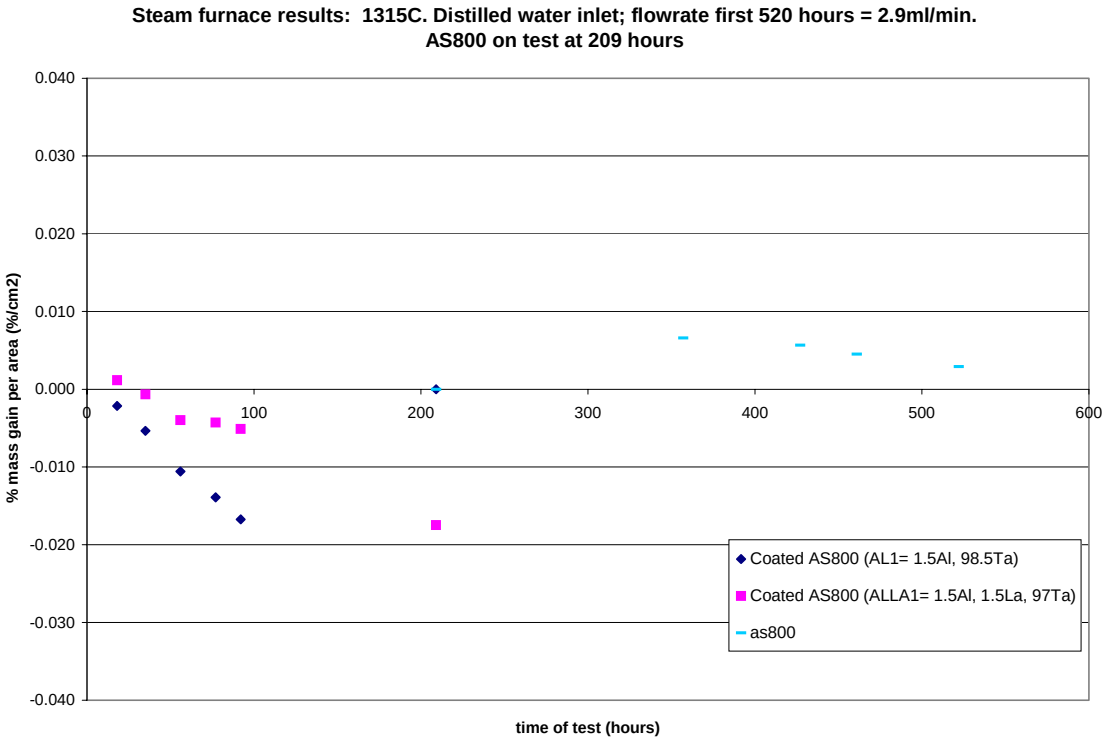

Figure 17. Weight gain as a function of time at 1315°C in Honeywell's steam furnace.

After the coated specimens were removed due to delamination, an AS800 specimen of approximately the same size with one surface "As-fired" was put into the furnace and was run for approximately another 300 hours. The mass change for the AS800 specimen is also shown in Figure 17. However, unlike the coated AS800 specimens, the uncoated AS800 had not been previously heat treated to 1250°C for 0.5 h (to stabilize the oxynitride grain boundary phases), nor had it been thermal cycled to 1200°C/1315°C for 1000/1000 cycles, respectively. (For the

coated specimens, the total time at temperature prior to water vapor testing was approximately 0.5h at 1250°C (before being coated), 416 hours at 1200°C (coated), and 416 hours at 1315°C (coated)).

After completion of the test, the steam-exposed coated and uncoated AS800 specimens were sent to Northwestern for further study and archiving.

3.4 Keiser Rig Testing

Eight pure Ta_2O_5-coated AS800 substrates were provided to Oak Ridge National Laboratory for Keiser Rig testing at 1315°C and 3% H_2O for 500 hours. These tests showed that undoped Ta_2O_5 is not an effective barrier at preventing sub-coating chemical changes to the AS800 substrate. Ta_2O_5-coated samples containing Al_2O_3 and La_2O_3 were also tested in the Keiser Rig. Reports of these studies are filed with DOE independently.

4. Additional Studies

Plasma-sprayed samples of pure Ta_2O_5 on AS800 were supplied to J.P. Singh of Argonne National Laboratory for indentation and fracture studies. Dr. Singh's reports his results to DOE under a separate contract.

CONCLUSIONS AND RECOMMENDATIONS

The major findings and accomplishments of the work as a result of the cooperative efforts among Northwestern University, Honeywell, Lehigh University and Oak Ride National Laboratory, are as follows:

- Conditions for the plasma spray of Ta_2O_5 and its alloys were optimized to provide maximum density (reflecting impermeability) and thickness (reflecting spray efficiency).
- Adherent small particle plasma spray (SPPS) coatings of doped and undoped Ta_2O_5 can be routinely prepared.
- Ta_2O_5 can be stabilized against its disruptive phase transformation up to temperatures of approximately 1400°C by the addition of one or more oxides of Al, La, and/or Nb.
- Residual stresses, which exist in the Ta_2O_5 coatings due to thermal expansion mismatch between coating and substrate, were measured using X-ray techniques and were found to change as a result of thermal exposure.
- Properly doped SPPS coatings are more resistant against thermal cycling than undoped coatings, and properly doped samples can be rapidly thermal cycled many thousand times without coating spallation.
- Water vapor testing in the ORNL Keiser rig of adherent undoped coating, which had not been thermally cycled, showed that undoped Ta_2O_5 is not an effective barrier at preventing sub-coating chemical changes to the AS800 substrate. (Reported by ORNL)
- Limited water vapor testing at Honeywell of selectively doped and adherent coatings, which had successfully survived many thermal cycles, showed that in the water vapor environment, de-cohesion may occur.

During the course of this program, the team has shown that Ta_2O_5 alloys are capable of being stabilized at all temperatures below 1400°C, and that certain Ta_2O_5 alloys when plasma-sprayed using SPPS on AS800 are capable of extended thermal cycling in air without significant delamination. However, from the Keiser rig results and from the Honeywell steam furnace test, it appears that Ta_2O_5, Ta_2O_5 + 1.5%Al_2O_3, and Ta_2O_5 + 1.5%Al_2O_3 + 1.5%La_2O_3 are not by themselves protective against environmental degradation of the AS800 at coating interface. However, as the thermal expansion of Ta_2O_5 is well matched to silicon-based ceramics, Ta_2O_5 alloys may be of use as part of a multilayer thermal barrier coating system.

Recommendations for future work

Future work to find an environmental barrier coating for silicon ceramics based on Ta_2O_5 might seek to find other dopants which stabilize Ta_2O_5 while providing lower oxide and water vapor transport. Additionally, as the thermal expansion of some Ta_2O_5 alloys is well matched to silicon-based ceramics, these alloys may be of use as part of a multilayer thermal barrier coating system. Other candidates for low water vapor transport should be explored.

Appendix A: Personnel Associated with the Project

Northwestern University personnel who participated in the effort

Katherine Faber	Principal investigator and Professor of Materials Science and Engineering
Chad Franks	Undergraduate, senior project (now employed at Boeing)
D. Lynn Johnson	Professor Emeritus of Materials Science and Engineering, provided advice regarding statistical design of experiments at no cost to the project
Monica Moldovan	Postdoctoral fellow (now employed at Louisiana State University
Christopher Weyant	Ph.D. student (now employed at Sandia National Laboratory)

Honeywell personnel who participated in, or who were cognizant of the activities undertaken include the following:

Jim Guiheen	Current Honeywell Project Director
Chien-Wei Li	Previous Honeywell Project Director
Eric Passman	Research engineer involved with powder synthesis
Bjoern Schenk	Honeywell Engines Silicon Nitride technology leader
Derek Raybould	Leader of separately funded Honeywell-internal EBC development effort

Lehigh University personnel who participated in the effort

Helen Chan	Lehigh Project Director and Professor Materials Science and Engineering
Martin Harmer	Professor of Materials Science and Engineering
Suxing Wu	Postdoctoral research associate

Additional personnel who donated time to the project

Jonathan D. Almer	Argonne National Laboratory, Advanced Photon Source

Appendix B: Papers and Presentations

1. "Tantalum Oxide Coatings as Candidate Environmental Barriers," M. Moldovan, C. M. Weyant, D. L. Johnson and K. T. Faber, *J. Thermal Spray Tech.* **13** [1] 51-56 (2004).

2. "Residual Stress and Microstructural Evolution in Tantalum Oxide Coatings on Silicon Nitride," C. M. Weyant, K. T. Faber, J. D. Almer, and J. V. Guiheen, to appear in *J. Amer. Ceram. Soc.*, 2005.

3. "Effect of Alumina Additions on Microstructural Aspects of the β to α Transformation in Tantalum (V) Oxide," S. Wu, H. M. Chan, and M. P. Harmer, submitted to the *J. Am. Ceram. Soc.*

4. "Residual Stress and Microstructural Evolution Environmental Barrier Coatings of Tantalum Oxide Alloyed with Alumina and Lanthana," C. M. Weyant, K. T. Faber, J. D. Almer, and J. V.Guiheen, in preparation for *J. Amer. Ceram. Soc.*

****

5. "Processing of Tantalum Oxide Small Particle Plasma-Sprayed (SPPS) Environmental Barrier Coatings for Use in Gas Turbine Engines," M. Moldovan, C.M. Weyant, and K.T. Faber, Annual Meeting of the American Ceramic Society, St. Louis, MO, April 2002.

6. "Residual Stress Analysis of Small Particle Plasma-Sprayed (SPPS) Tantalum Oxide Environmental Barrier Coatings," C.M. Weyant and K.T. Faber, Annual Meeting of the American Ceramic Society, St. Louis, MO, April 2002.

7. "Effects of Additives on Sintering Behavior of Tantalum Pentoxide," H.M. Chan, M.P. Harmer and S. Wu, Annual Meeting of the American Ceramic Society, St. Louis, MO, April 2002.

8. "Small Particle Plasma Spray Coatings fro Thermal and Environmental Barriers," K.T. Faber, 54th Pacific Coast Regional Meeting and Basic Science Division Meeting, Seattle, WA, September 2002 (invited paper).

9. "Tantalum Oxide-Bases Environmental Barrier Coatings," J. V. Guiheen, C.-W. Li, H.M. Chan, M.P. Harmer, S. Wu, K. T. Faber, M. Moldovan, C. M. Weyant, M. Ferber and K. More, Environmental Barrier Coatings Workshop, Nashville, TN, November 2002 (invited talk).

10. "Residual Stress Analysis of Plasma Sprayed Tantalum Oxide-Based Environmental Barrier Coatings," C. M. Weyant, K. T. Faber, J. Almer, J. V. Guiheen, Annual Meeting of the American Ceramic Society, Nashville, TN, April 2003

11. "Tantalum Oxide Coatings for Environmental Barriers," K.T. Faber, M. Moldovan and C. Weyant, International Thermal Spray Conference 2003, Orlando, FL, May 2003.

12. "Phase and Microstructural Evolution in Plasma-Sprayed Tantalum Oxide-Based Environmental Barrier Coatings," C.M. Weyant, K T. Faber, J.V. Guiheen and J.D. Almer, Annual Meeting of the American Ceramic Society, Indianapolis, IN, April 2004.

13. "Tantalum Oxide EBCs for AS800," J. Guiheen, C.-W. Li, H. Chan, M. Harmer, S. Wu, K. Faber, M. Moldovan, C. Weyant, K. More, M. Ferber," Environmental Barrier Coatings Workshop, Nashville, TN, November 2003.

14. "Residual Stresses in Plasma-Sprayed Tantalum Oxide-Based Environmental Barrier Coatings, "C.M. Weyant, K.T. Faber, J.D. Almer, and J.V. Guiheen, Annual Meeting of the American Ceramic Society, Indianapolis, IN, April 2004.

15. "Tantalum Oxide-Based Environmental Barrier Coatings," K. T. Faber, C. M. Weyant, J. Almer and J.V. Guiheen, 5th International Conference on High-Temperature Ceramic Matrix Composites, Seattle, WA September, 2004. (invited paper)

Appendix C: Honeywell Thermal Cycling Test Facilities

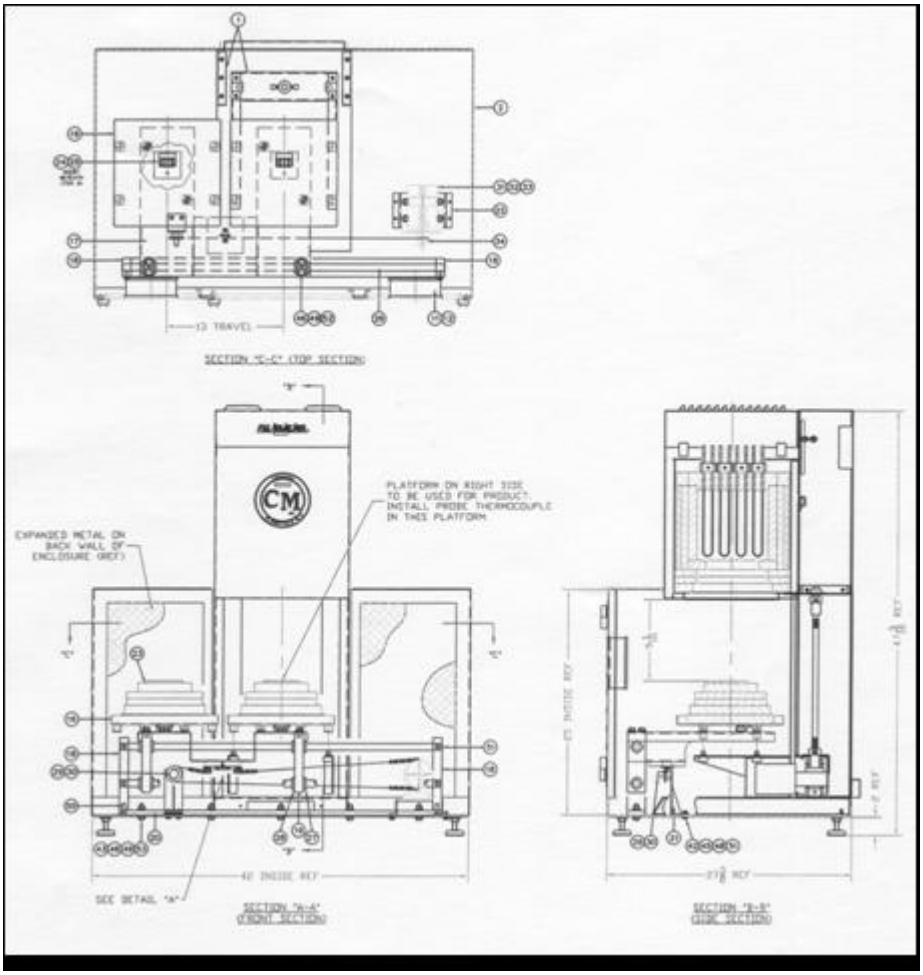

CM Furnaces Model 1708 BL with cycling option
- T_{max} = 1700°C
- Type B control & O/T thermocouples
- PLC position control and cycle logging
- Extra Monitoring T/C with output to analog chart recorder
- procured under Honeywell funds completely separate from DOE/Northwestern subcontract
- can accommodate samples within a 6” cube
- Room temperature to “at-temp” in 40 seconds
- “at-temp” to fan in 20seconds
- 25 minutes “at temp”, 5 minutes off
- Over 2500 cycles logged since February 2003

Appendix D: Summary log of thermal cycling samples for Round 1

Coating composition	**#cycles @ 1200°C**	**#cycles @ 1315°C**	**Results, observations**
Group X: Uncoated			
sample X1	139		No noticeable visual change
sample X2	489		No noticeable visual change
sample X3	986		No noticeable visual change
sample X4	1074		No noticeable visual change
Group A: Pure Ta_2O_5			
sample A1	139		Delamination seen
sample A2	489		No delamination seen
sample A3	489		No delamination seen
sample A4	986		No delamination seen
sample A5	1074		No delamination seen
sample A6	1074		No delamination seen
sample A7: second population	100	1325	Edges beginning to delam
Group B: Ta_2O_5 + 5%Al_2O_3			
sample B1	139		Delaminated
sample B2	489		Delaminated
sample B3	489		Delaminated
sample B4	986		Delaminated
sample B5	1074		Delaminated
sample B6	1074		Delaminated
sample B7	1074		Delaminated
Group C: Ta_2O_5 + 2%Al_2O_3			
sample C1	145		No delamination seen
sample C2	489	2033	No delamination seen at 1500 cycles. Delamination noted at 1700 cycles
sample C3: second population	100	1325	No delam. seen by Guiheen. Severe edge delam. seen by Weyant
Group D: Ta_2O_5 + 3%Al_2O_3 + 3%La_2O_3			
sample D1	145		No delamination seen
sample D2	489		No delamination seen
sample D3: second population	100	3358	No delamination seen
Group E: Ta_2O_5 + 3%Al_2O_3			
sample E1	100	3358	No delam. seen at 2825 cycles. Delamination at 3025 cycles

Appendix E: Summary log of thermal cycling samples for 2nd group of samples

Coating composition	**#cycles @ 1200°C**	**Results, observations**
Group A': Ta_2O_5 + 1.5wt% Al_2O_3		
sample A'1	140	No delamination seen
sample A'2	490	No delamination seen
sample A'3	1080	No delamination seen
Group B': Ta_2O_5 + 1.5wt% Al_2O_3		
sample B'1	140	No delamination seen
sample B'2	490	No delamination seen
sample B'3	1080	No delamination seen
Group C': Ta_2O_5 + 1.5wt% Al_2O_3 + 1.5% La_2O_3		
sample C'1	140	No delamination seen
sample C'2	490	No delamination seen
sample C'3	1080	No delamination seen
Group D': Ta_2O_5 + 1.5wt% Al_2O_3 + 1.5% La_2O_3		
sample D'1	140	No delamination seen
sample D'2	490	No delamination seen
sample D'3	1080	No delamination seen
Group E': Ta_2O_5 + 1.5wt% Al_2O_3		
sample E'1	140	No delamination seen
sample E'2	490	No delamination seen
Group E': Ta_2O_5 + 1.5wt% Al_2O_3		
sample F'1	140	No delamination seen
sample F'2	490	No delamination seen